REMOTE SENS. ENVIRON. 41:133-142 (1992)

Modeled Analysis of the Biophysical Nature of Spectral Shifts and Comparison with Information Content of Broad Bands

F. Baret, S. Jacquemoud, and G. Guyot
INRA, Bioclimatologie, Montfavet, France
C. Leprieur
LERTS, Toulouse, France

Spectral shifts characterized by the wavelength λ_i of the inflexion point in the red-edge region (670–780 nm) are analyzed using model simulations. Leaf optical properties are computed with the PROSPECT model, canopy reflectance with the SAIL model, and atmospheric effects with the 5S model. The information provided by the high spectral resolution index (λ_i) appears to be equivalent to that obtained from the red and near-infrared broad band reflectances at leaf level. This is not true at canopy level: λ_i is very sensitive to leaf area index and chlorophyll concentration and, when observed from space sensors, it minimizes the effects of atmosphere and soil background optical properties. Moreover, λ_i could be a pertinent indicator of canopy photosynthetic capacity. But its small dynamic range requires further studies in which sensor noise has to be considered, depending on the method of λ_i computation.

INTRODUCTION

Present developments of spectro-imaging sensors such as AIS (Airborne Imaging Spectrometer), AVIRIS (Airborne Visible Infrared Imaging Spectrometer), or MODIS (Moderate resolution Imaging Spectrometer) (Slater, 1986) require a simultaneous research effort in the interpretation of this new remotely sensed information. For biosphere applications, various studies have been carried out to explain the spectral features observed either at the leaf scale or on canopies sensed from space. Most of the work focuses on the red edge (650–800 nm) where the optical properties change sharply with wavelength (Horler et al., 1983). First or second derivatives of the spectra with respect to the wavelength (Demetriades-Shah and Steven, 1988; Hall et al., 1990) and spectral shifts of the inflexion point of the red edge (Baret et al., 1987; Belanger, 1990; Chang and Collins, 1983; Collins et al., 1983; Ferns et al., 1984; Gauthier and Neville, 1985; Horler et al., 1983; Leprieur, 1989; Miller et al., 1985) are generally used to describe the spectral features. As for broad band vegetation indices, these spectral features have been related to leaf or canopy characteristics.

At leaf level, the spectral features observed in the red edge are related to chlorophyll or other absorbing pigments concentrations as well as to the mesophyll internal structure (Belanger, 1990; Curran et al., 1991; Gates et al., 1965; Guyot et

Address correspondence to F. Baret, INRA—Bioclimatologie, BP 91, 84143 Montfavet Cedex, France.
Received 1 March 1992.

0034-4257/92/$5.00

655 Avenue of the Americas, New York, NY 10010

al., 1991; Horler et al., 1983). An increase in chlorophyll concentration shifts the inflexion point towards longer wavelengths and increases the absolute value of the first and second derivatives. At canopy level, these spectral features have been correlated with stress or chlorosis induced by high concentrations of heavy metals (Chang and Collins, 1983; Collins et al., 1983; Demetriades-Shah and Steven, 1988; Gauthier and Neville, 1985; Miller et al., 1985; Milton and Mouat, 1989; Rock et al., 1990) or, in more general terms, with vegetation vigor status (Baret et al., 1987; Boochs et al., 1990). But, at canopy level, many external factors induce noise in the relationships observed at leaf level and complicate the interpretation of the spectral features (Curran et al., 1991; Guyot et al., 1991; Vanderbilt et al., 1988). More recently, some authors justify, in an opposite way, the use of the spectral features because it minimizes the noise induced by some factors such as soil optical properties (Demetriades-Shah et al., 1990; Hall et al., 1990). However, few studies (Price, 1990) consider the real gain in information content of the data provided by spectro-imaging systems as compared with the classical broad bands.

This article is an attempt to analyze the sensitivity of the spectral feature both at leaf and canopy scales using modeled output. We will more particularly focus on the spectral shifts characterized by the wavelength of the inflexion point λ_i, in the red edge domain. We will evaluate the advantages of using this kind of high spectral resolution index compared to the use of classical wide bands. These analyses will be based on leaf and canopy reflectance models. We will finally address issues linked to satellite observations and the atmospheric effects.

EQUIVALENCE BETWEEN λ_i AND WIDE BAND REFLECTANCES AT LEAF LEVEL

We have used the PROSPECT model (Jacquemoud and Baret, 1990) to simulate leaf optical properties as a function of their biophysical properties. In this simple modeling approach, scattering is produced by refractive index variations at each interface between air and leaf material. The leaf mesophyll internal structure is thus described by the number of interfaces characterized by the parameter N. Since the refractive index of leaf material, $n(\lambda)$, varies only slightly with wavelength, the spectral edges are due to absorption features. The absorption is characterized by an absorption coefficient $[K(\lambda)]$, which is the product of a specific absorption coefficient $[k(\lambda)]$, strongly dependent on the wavelength, and the concentration (C) of the absorbing material:

$$K(\lambda) = \sum_i k_i(\lambda) C_i. \quad (1)$$

We will consider explicitly only chlorophyll *a* and *b* pigments (characterized by $k_{ab}(\lambda)$ and C_{ab}) and water ($k_w(\lambda)$ and C_w). This simple case allows the computation of realistic leaf reflectance and transmittance spectra in the optical domain using only three input variables, which are not wavelength dependent: C_{ab}, C_w, and N. As the absorption domains of water and chlorophyll are distinct, we have described each part of $k_{ab}(\lambda)$ or $k_w(\lambda)$ curves by sigmoïdal curves:

$$k(\lambda) = \alpha_1(\alpha_2 + (1 - \alpha_3 e^{-\alpha_4(\lambda - \alpha_5)})^{\alpha_6}). \quad (2)$$

The different α values are reported in Table 1 for certain spectral domains where an "edge" can be observed. These analytical expressions of $k(\lambda)$ are used to formally derive the PROSPECT model in order to determine the position of the inflexion point from leaf reflectance or transmittance in various spectral domains. In the red edge, we obviously observe the strong dependence of λ_i on chlorophyll concentration, but it also depends on the mesophyll internal structure through the N parameter (Fig. 1). The λ_i values range from 683 nm for low chlorophyll concentrations, to a maximum of 715 nm for thick green leaves with a spongy mesophyll ($N > 2.0$). The relationships between λ_i and total chlorophyll agree with the experimental results obtained by Belanger (1990) on deciduous tree species and Horler et al. (1983)

Table 1. α Values for Eq. (2) in Four Spectral Domains[a]

	k_{ab}		k_w	
	452–458	*672–752*	*1340–1446*	*1800–1922*
α_1	−0.0239	−0.0317	18.0795	55.2895
α_2	−1.3020	−1.0000	0.1182	0.1021
α_3	−21.4672	0.9396	−0.5505	−16.8349
α_4	0.1588	0.0982	0.0609	0.0990
α_5	491.2	672.0	1371.8	1864.1
α_6	−0.4806	2.9942	−7.7388	−0.7681
λ_i	505.9	682.5	1395.6	1889.9

[a] λ_i is the position of the inflexion point of the specific absorption coefficient $k(\lambda)$. The wavelengths are in nm and $k(\lambda)$ in μg^{-1} cm^2.

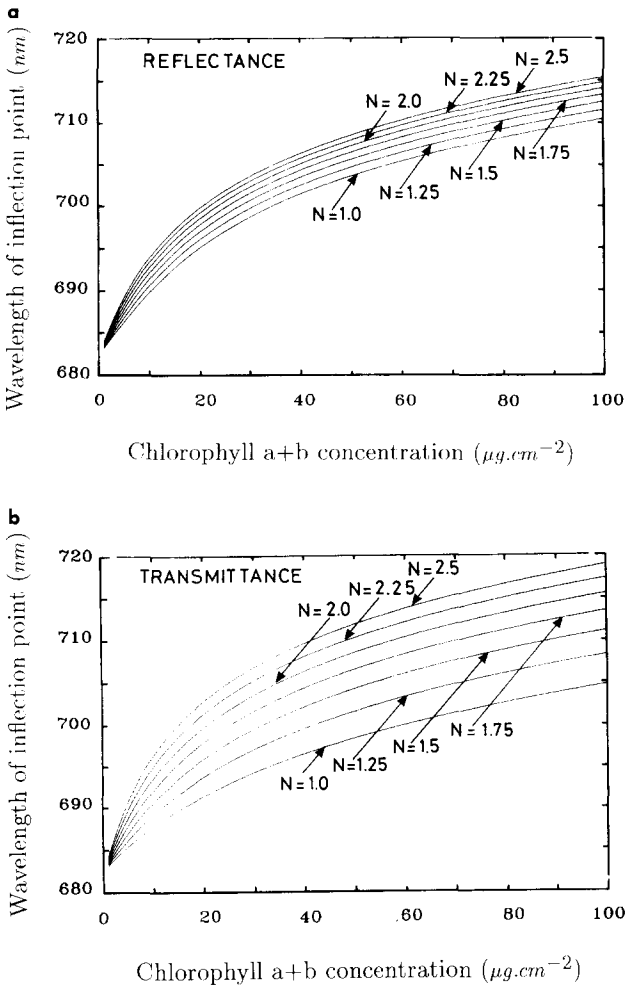

Figure 1. Sensitivity of λ_i to chlorophyll concentration (C_{ab}) and mesophyll internal structure parameter (N).

on dicotyledonous tree species and monocotyledonous cereals. Similar behavior is observed in the blue-green domain (452–548 nm) as a function of the chlorophyll concentration (C_{ab}) and in the middle infrared (1340–1446 nm and 1800–1922 nm) as a function of the equivalent water thickness (C_w).

As the spectral absorption domains of water and chlorophyll pigments do not overlap, leaf optical properties are fully explained by only two input variables (C and N) in a particular spectral domain (visible-near infrared or near-middle infrared). Inside one of these spectral domains, two narrow wavebands (λ_1 and λ_2) should be theoretically sufficient to invert the PROSPECT model from reflectance or transmittance values and retrieve the C and N variables. Thus, they should allow computation of the corresponding λ_i. In consequence, a one-to-one function F should relate the spectral shift λ_i to the reflectance (or transmittance) data set $(\rho(\lambda_1),\rho(\lambda_2))$:

$$\lambda_i = F(\rho(\lambda_1),\rho(\lambda_2)). \quad (3)$$

In the red edge, λ_i is very accurately fitted (RMSE = 0.73 nm) by a polynomial surface of the fourth order in $\rho(672)$ (maximum absorption wavelength) and $\rho(780)$ (near-infrared plateau) that represents the F function. From a statistical point of view, this confirms the equivalence between the reflectances in two wavebands and the spectral shift. Due to the smooth variation in a restricted spectral domain around 672 nm and 780 nm, there are little differences between the broad band reflectances in the red and near infrared (LANDSAT or SPOT bands, for example), and the high spectral reflectances $\rho(672)$ and $\rho(780)$. Thus, we conclude that, at the leaf level, red and near infrared reflectances have an equivalent information content as the spectral shifts.

ANALYSIS AT CANOPY LEVEL

Canopy Biophysical Characteristics and λ_i

Canopy reflectance spectra are simulated using the PROSPECT model from which leaf reflectance and transmittance spectra are fed into the SAIL canopy reflectance model (Verhoef, 1984; 1985). Near the red edge, the spectral reflectance of the canopy $\rho(\lambda)$ is a function R_l of

$$\rho(\lambda) = R_l(n(\lambda),k_{ab}(\lambda),C_{ab},N,l,\theta_o,\phi_o,\theta_s,\theta_l,\rho_s(\lambda)), \quad (4)$$

where l is the leaf area index, θ_o and ϕ_o are the view zenith and azimuth angles, θ_s is the sun zenith angle (90% of the incoming energy is assumed to be in the sun direction, the remaining 10% corresponding to a diffuse flux), θ_l is the average leaf angle inclination (we have considered ellipsoidal distributions) (Campbell, 1986; Wang and Jarvis, 1988), and $\rho_s(\lambda)$ is the soil spectral reflectance. We split the input variables of the canopy reflectance function R_l into spectrally dependent (mainly k_{ab} and ρ_s) and non-spectrally dependent. Following the results of Bowers and Hanks (1965) or Stoner and Baumgardner (1985), we will assume a linear variation of the soil reflectance near the red edge. Using the soil line concept between the red (672 nm) and the near

infrared (780 nm) (Baret and Guyot, 1991; Richardson and Wiegand, 1977), we propose a single empirical relationship between the soil reflectance ρ_s and both the wavelength (λ) and a brightness index which could be the soil red reflectance [$\rho_s(672)$]:

$$\rho_s(\lambda) = \rho_s(672) + \frac{\lambda - 672}{780 - 672}(0.2\rho_s(672) + 0.04). \quad (5)$$

We will thus define the R_2 function as

$$\rho(\lambda) = R_2(\lambda, X), \quad (6)$$

where $X = (c_{ab}, N, l, \theta_o, \phi_o, \theta_s, \theta_l, \rho_s(672))$ is the vector of the spectrally independent input variables. Expression (6) allows the second derivative $[d^2\rho(\lambda)/d\lambda^2]$ to be formally calculated and thus λ_i to be determined by setting $d^2\rho(\lambda)/d\lambda^2 = 0$. For simplicity, we will only present simulations performed at the nadir ($\theta_o = 0$). As the leaf index is one of the most important variables governing canopy processes, we will always analyse the sensitivity of each other input variable in interaction with l. The spectral shifts are primarily governed both by the chlorophyll concentration and the leaf area index (Fig. 2). Any increase of the chlorophyll concentration or of the leaf area index shifts λ_i towards longer wavelengths. This is in good agreement with experimental results observed by Demetriades-Shah and Steven (1988) or Rock et

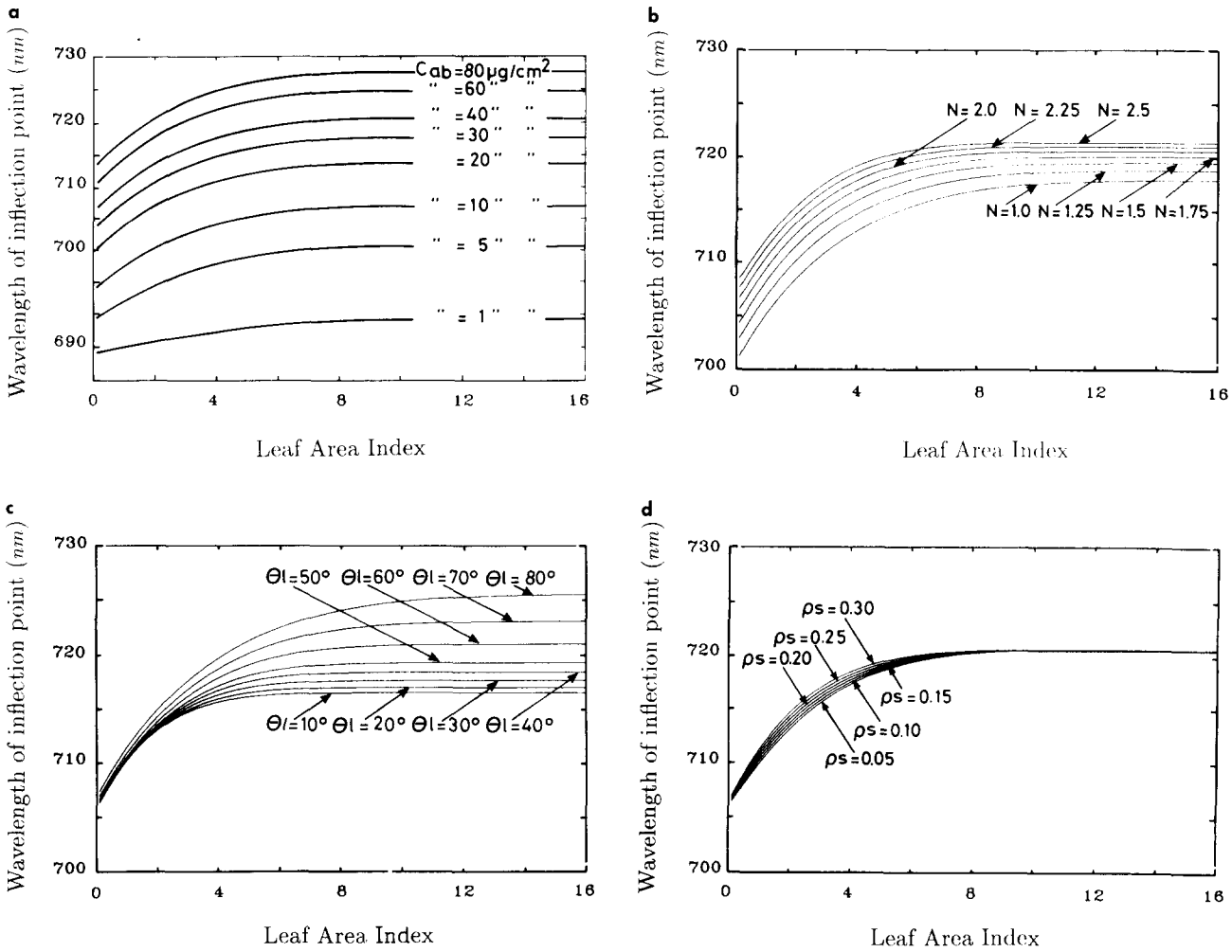

Figure 2. Sensitivity of λ_i to leaf area index l, chlorophyll concentration C_{ab}, the mesophyll internal structure parameter N, canopy architecture θ_l and soil optical properties $\rho_s(672)$. Angles are in degrees. a) Variation with l and (C_{ab} for $X = C_{ab}$, l,0,0,40,58,0.15); b) variation with l and N for $X = (40,N,l,0,0,40,58,0.15)$; c) variation with l and θ_l for $X = (40,2,l,0,0,40,\theta_l, 0.15)$; d) variation with l and $\rho_s(672)$ for $X = (40,2,l,0,0,40,58,\rho_s(672))$.

al. (1988). The range of λ_i variation for canopies is close to that reported for individual leaves, considering the full range of variation of chlorophyll concentration. However, for a given chlorophyll concentration, the dynamics of λ_i is reduced to a maximum of 20 nm. Canopy architecture effects (θ_l) are significant: This has been confirmed by Vanderbilt et al. (1988), who showed that changes in the geometric structure of the plant canopy, due to the wind, may induce red edge shifts, especially for erect canopies. The effect of the mesophyll internal structure is also significant: When the N parameter increases from 1.0 to 2.0, λ_i shifts about 4 nm towards longer wavelengths. The spectral shifts in the red edge are nearly independent of the soil background optical properties. Complementary simulations show a very small influence of irradiance conditions on λ_i (sun position, diffuse fraction).

Spectral shifts in the red edge seem to be particularly sensitive to input variables that govern the photosynthetic activity of the canopy such as chlorophyll concentration, leaf area index, or canopy architecture (Charles-Edwards, 1982). It will be interesting to relate this high spectral resolution index to more global biophysical variables such as the whole canopy chlorophyll content or the efficiency of the canopy in trapping photosynthetically active radiation, as suggested by Hall et al. (1990). Furthermore, λ_i minimizes the influence of uncontrolled variables such as soil optical properties. Among the input variables, we can then distinguish those we want to assess from remote sensing data and those in which we have no interest and producing noise in the retrieved variables (we can denote them Θ). We propose to look for the conditions on the last category of input variables Θ so that λ_i does not depend on Θ. For this purpose, we define the function g as the second derivative of the canopy reflectance with respect to the wavelength: $g = d^2\rho(\lambda)/d\lambda^2$. This function depends on the wavelength and on other input variables including Θ: $g = g(\lambda,\Theta)$. We can define the implicit function $\lambda_i(\Theta)$ such as $g(\lambda_i,\Theta) = 0$. The basic properties of implicit functions lead to

$$\frac{d\lambda_i}{d\Theta} = -\frac{dg}{d\Theta}\Big/\frac{dg}{d\lambda}. \tag{7}$$

This equation states that the independence of λ_i with respect to the input variable Θ is equivalent to the independence of the second derivative g with respect to Θ ($d\lambda_i/d\Theta = 0 \Leftrightarrow dg/d\Theta = 0$). Let us assume that the input variable Θ depends on the wavelength: $\Theta = \Theta(\lambda)$. This corresponds, for example, to the case of the soil reflectance. Canopy spectral reflectance can be expressed in the form $\rho = \rho(\Omega(\lambda),\Theta(\lambda))$, where Ω corresponds to the input variables distinct from Θ. The Ω input variables include those we want to retrieve from high spectral resolution indices, such as the chlorophyll content, the leaf area index, or other variables which may depend on the wavelength such as the irradiance conditions. With those definitions, we can express the second derivative g of canopy reflectance with respect to the wavelength:

$$g = \frac{d^2\rho}{d\Theta^2}\left(\frac{d\Theta}{d\lambda}\right)^2 + \frac{d\rho}{d\Theta}\frac{d^2\Theta}{d\lambda^2} + \frac{d^2\rho}{d\Omega^2}\left(\frac{d\Omega}{d\lambda}\right)^2 + \frac{d\rho}{d\Omega}\frac{d^2\Omega}{d\lambda^2}. \tag{8}$$

If we differentiate g with respect to Θ, we have

$$\frac{dg}{d\Theta} = \frac{d^3\rho}{d\Theta^3}\left(\frac{d\Theta}{d\lambda}\right)^2 + 3\frac{d^2\rho}{d\Theta^2}\frac{d^2\Theta}{d\lambda^2} + \frac{d\rho}{d\Theta}\frac{d\lambda}{d\Theta}\frac{d^3\Theta}{d\lambda^3} + \frac{d\Omega}{d\Theta}\left[\frac{d^3\rho}{d\Omega^3}\left(\frac{d\Omega}{d\lambda}\right)^2 + 3\frac{d^2\rho}{d\Omega^2}\frac{d^2\Omega}{d\lambda^2} + \frac{d\rho}{d\Omega}\frac{d\lambda}{d\Omega}\frac{d^3\Omega}{d\lambda^3}\right]. \tag{9}$$

As by definition Ω is independent of Ω ($d\Omega/d\Theta = 0$, Eq. (9) simplifies and gives the condition under which g, and thus λ_i, do not depend on the parameter Θ:

$$\frac{d^3\rho}{d\Theta^3}\left(\frac{d\Theta}{d\lambda}\right)^2 + 3\frac{d^2\rho}{d\Theta^2}\frac{d^2\Theta}{d\lambda^2} + \frac{d\rho}{d\Theta}\frac{d\lambda}{d\Theta}\frac{d^3\Theta}{d\lambda^3} = 0. \tag{10}$$

In particular, this condition is obtained when

$$\frac{d^2\rho}{d\Theta^2} = 0$$

and

$$\frac{d^2\Theta}{d\lambda^2} = 0. \tag{11}$$

Conditions (11) are thus obtained when the canopy reflectance is a linear fraction of the input variable Θ, and when Θ varies linearly with wavelength on the spectral domain considered. For example, the canopy reflectance can be approximated by a linear function of soil reflectance (Baret, 1988), and soil reflectance spectra are

quasilinear with wavelength in the red edge as discussed earlier. These two properties correspond to conditions (11) and explain why λ_i is not influenced by soil optical properties (Fig. 2d).

In this section, we have established the biophysical meaning of the spectral shifts which gives some credence to the use of these high spectral resolution indices. However, we still have to compare this information derived from high spectral resolution sensors with that obtained with classical wide bands.

Relationships between λ_i and Red and Near-Infrared Reflectances

As seen earlier, at ground level, canopy reflectance spectra, in a given spectral domain, depend only on a limited set of input variables. Consequently, a strong redundancy is expected among the different reflectances observed along the spectrum. Similarly to our study at leaf level, we will evaluate which is the new information carried by λ, as compared to that obtained from classical broad wavebands.

We have built a very large set of simulated λ_i, $\rho(672)$, and $\rho(780)$ values using the PROSPECT and SAIL models. The input variable vectors X are randomly drawn, considering the following independent distributions of each individual input variable: uniform distribution for N ($1 \leqslant N \leqslant 2.5$), θ_o ($0° \leqslant \theta_o \leqslant 60°$), ϕ ($0° \leqslant \phi \leqslant 180°$), θ_s ($20° \leqslant \theta_s \leqslant 70°$), θ_l ($20° \leqslant \theta_l \leqslant 80°$), and $\rho_s(672)$ ($0.1 \leqslant \rho_s(672) \leqslant 0.30$); lognormal distributions for C_{ab} ($0.1 \leqslant C_{ab} \leqslant 80$ μg cm^2) and l ($0.1 \leqslant l \leqslant 16$). The latter choice is explained by the previous analysis, which highlights the large sensitivity of λ_i to low values of C_{ab} or l.

The surface corresponding to the polynomial approximation of λ_i as a function of $\rho(672)$ and $\rho(780)$ is not as smooth (RMSE = 5.2 nm) as that observed for leaves. In some particular configurations, the same red and near infrared reflectances may correspond to different λ_i values (Fig. 3). These results demonstrate that the spectral shifts in the red edge are not strictly equivalent to the red and near-infrared reflectances. However, the accuracy of λ_i, as explained by single waveband reflectances using the same polynomial fitting techniques, increases drastically with the number of wavebands. When a narrow waveband centered at 710 nm between red and near-infrared bands is added, the RMSE of λ_i decreases to 1.6 nm; but when we add new complementary wavebands, they must be narrow, and we have to pay attention to gaseous absorption features which may restrict the use of a large number of wavebands. This naturally leads us to address the issue of atmospheric effects, and more generally to study problems related to space observations.

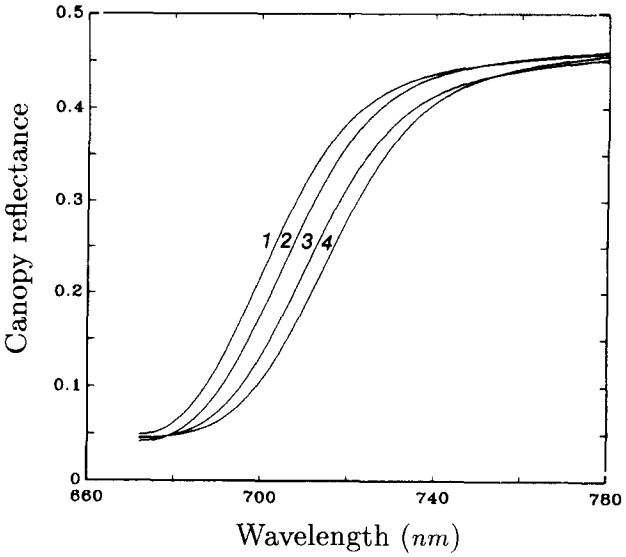

Figure 3. Spectra simulated with the same red and near infrared reflectances, but with differing λ_i values. 1) X = (8.8, 2.43, 1.58, 54.5, 163.3, 66.6, 72, 0.22); 2) X = (46.5, 2.5, 1.2, 31, 27.8, 67, 45, 0.25); 3) X = (35.5, 2.27, 1.02, 48, 1.8, 69.3, 74.6, 0.18); 4) X = (17.9, 1.78, 1.9, 37.6, 106.8, 60.1, 44.9, 0.20).

PROBLEMS RELATED TO SPACE OBSERVATIONS

Atmospheric Effects

Apparent reflectances at satellite level ρ_* can be simply related to the target reflectance ρ when the surrounding optical properties are similar (Conel et al., 1988):

$$\rho_* = u\rho + v. \tag{12}$$

The second derivative of ρ with respect to the wavelength is then

$$\frac{d^2\rho_*}{d\lambda^2} = 2\frac{du}{d\lambda}\frac{d\rho}{d\lambda} + u\frac{d^2\rho}{d\lambda^2} + \rho\frac{d^2u}{d\lambda^2} + \frac{d^2v}{d\lambda^2}. \tag{13}$$

Simulations performed with the 5S model (Tanré

et al., 1990) show that, outside gaseous absorption bands, the u and v parameters are quasilinear functions of the wavelength ($d^2u/d\lambda^2 \approx 0$ and $d^2v/d\lambda^2 \approx 0$) (Fig. 4). Furthermore, the increase of u with respect to the wavelength is very small ($du/d\lambda^2 \approx 0$). Equation (13) is thus approximated by

$$\frac{d^2\rho^*}{d\lambda^2} \approx u\frac{d^2\rho}{d\lambda^2}. \qquad (14)$$

This clearly shows that, for a given sensor, ground level spectral shifts (λ_i) are equivalent to the ones observed from space (λ^*_i), taking into account the atmospheric effects. Numerical simulations confirm the interesting properties of this high spectral resolution index as compared to the second derivative, affected by atmospheric characteristics through the parameter u, or to the use of classical broad bands, vegetation indices such as the NDVI (Fig. 5).

However, though it may be easy to compute λ_i from model simulations or to calculate it from high spectral resolution measurements acquired at ground level, the problem is much more complex when evaluating λ_i from spectro-imaging systems on airborne or space platforms.

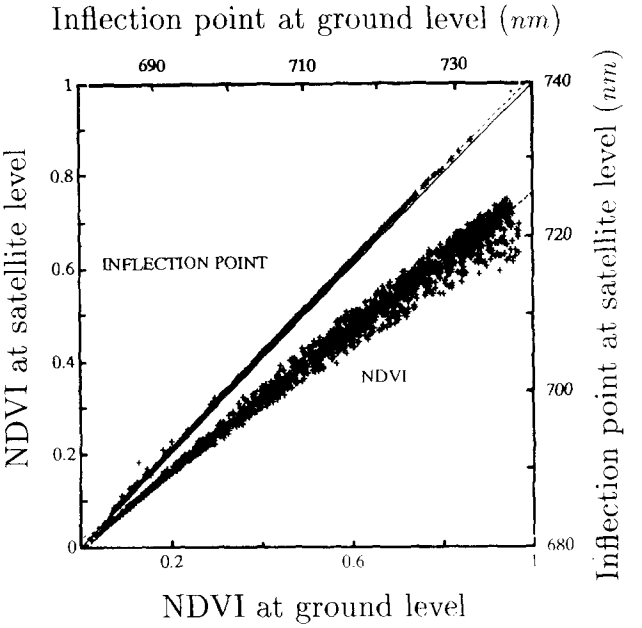

Figure 5. Relationship between ground level and satellite level spectral indices λ_i and NDVI. The data are simulated as described in the text, using the random drawing procedure for X input variables values, but restricted to nadir viewing, with a sun zenith angle of 40° and a diffuse fraction of 0.4 corresponding to the atmospheric conditions described in Figure 4. The satellite signal is simulated using the 5S model with the atmospheric characteristics described above.

Procedures Used to Evaluate λ_i from Space Observations

Three main constraints apply to the method of computation of λ_i from data recorded by high spectral resolution space-based sensors: i) gaseous absorption which requires particular corrections or the use of limited portions of the red edge domain (705–715 nm; 732–737 nm; 743–756 nm; 772–780 nm); ii) the number of spectral bands available and the corresponding computation time needed by the algorithm; iii) the noise associated with the sensor (spectral and radiometric), the minimization of which requires an increase in the number of wavebands. Using these criteria, we can divide λ_i computation procedures into three main groups:

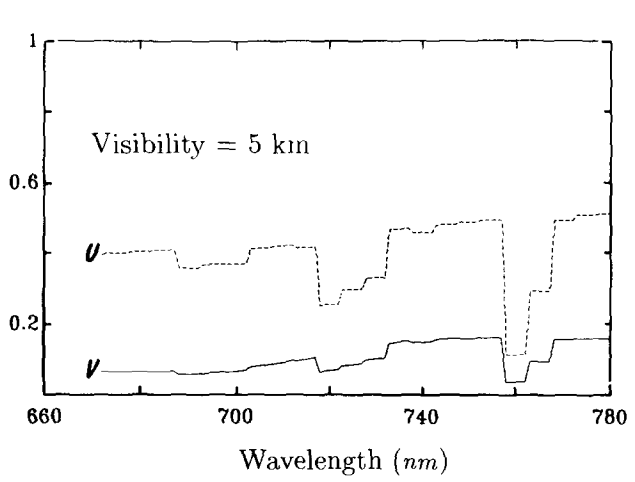

Figure 4. Spectral variation of parameters u and v [Eq. (12)] as simulated by the 5S model for a 5 km visibility and a midlatitude continental atmosphere. The three main dips at 650 nm, 730 nm, and 760 nm correspond to gaseous absorption features.

Smoothing and numerical derivation are mainly used for leaf or ground level canopy measurements when many narrow wavebands are available (Curran et al., 1990; Demetriades-Shah and Steven, 1988; Ferns et al. 1984; Milton and Mouat, 1989). Despite good results, this type of method is limited by the two first constraints.

Fitting the red edge to an empirical model allows the noise to be smoothed and allows λ_i to be derived analytically. Collins et al. (1983) uses a Cheybyshev orthogonal decomposition, but

Gauthier and Neville (1985) remark that it requires too many wavebands to be really applied to space data. Chang and Collins (1983), Miller et al. (1985), and Belanger (1990) use a gaussian model to fit the red edge. It needs three parameters and thus at least three wavebands to be fitted. However, this last technique is still time-consuming (Bonham-Carter, 1988) and not very realistic when compared to the true λ_i (Fig. 6).

Linear models: Because the red edge is quasilinear around the inflexion point, Gauthier and Neville (1985) characterize the spectral shifts by the intercept with the abscissa of the red edge approximated by a straight line. Baret et al. (1987) and Leprieur (1989) characterize λ_i by the wavelength of the point corresponding to the average reflectance between the red and the near-infrared wavebands, but, here again, this extreme simplification leads to serious errors (Fig. 7) which could distort the specific properties of this high spectral resolution index.

Against these different possibilities, we propose an alternative method that allows λ_i to be accurately evaluated from a limited set of wavebands: The polynomial fitting of λ_i as a function of the three $\rho(672)$, $\rho(710)$, and $\rho(780)$ narrow wavebands (Fig. 8), as reported earlier, is easy to handle, not very time-consuming, and accurate. Furthermore, we can adapt the method, according to the number of available wavelengths and computing capabilities. Despite its having been fitted to simulated data, this method can

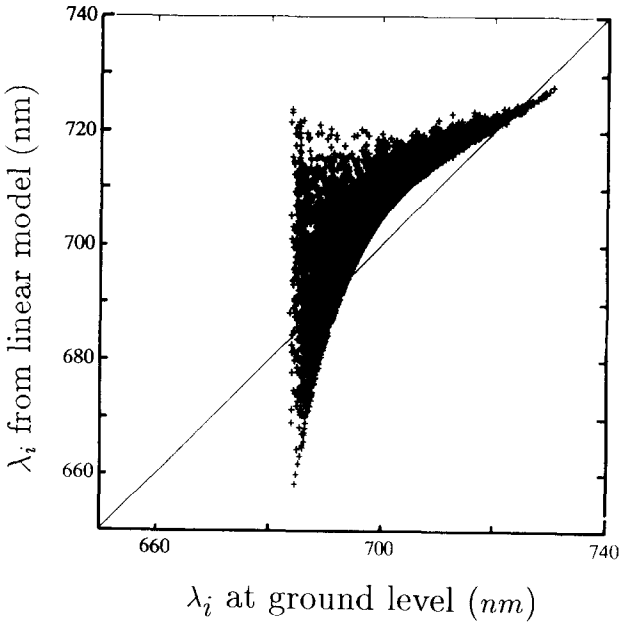

Figure 7. Same as Figure 6, but with λ_i estimated by the linear model.

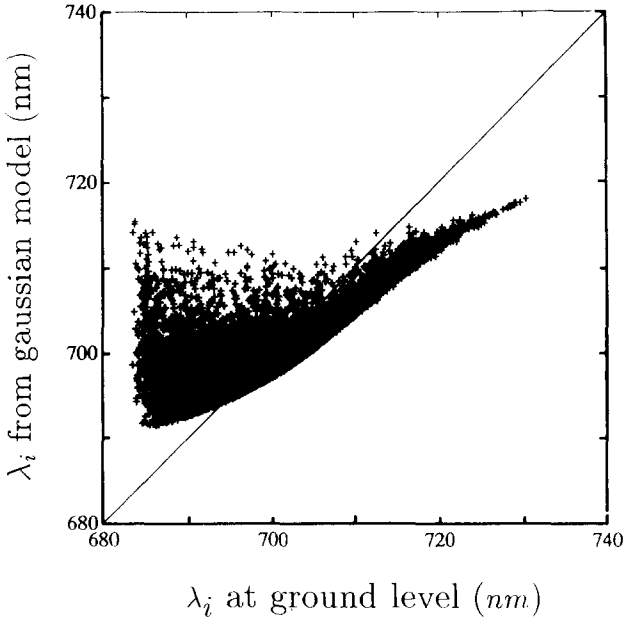

Figure 6. Relationship between λ_i estimated by fitting the gaussian model to the red edge, and the true λ_i calculated analytically. Results from canopy reflectance model simulations at ground level, with the same random drawing of input variables as described in previous sections.

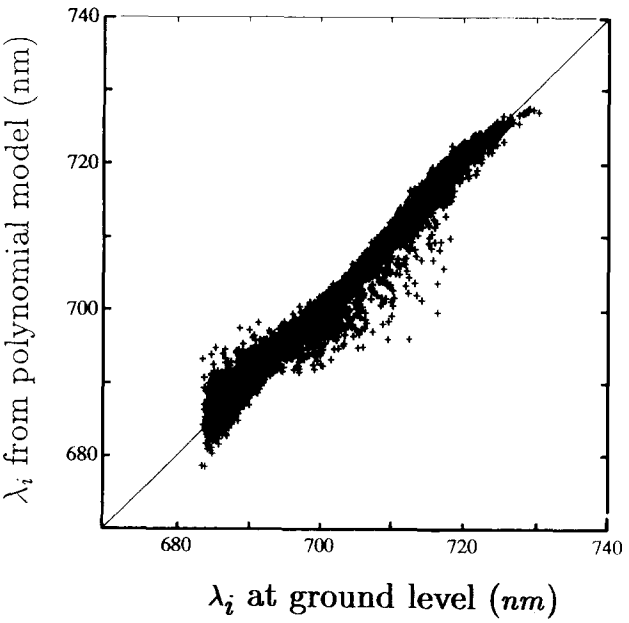

Figure 8. Same as Figure 6, but with λ_i estimated with the alternative polynomial fitting techniques using just three wavebands, $\rho(672)$, $\rho(710)$, and $\rho(780)$.

also be applied to high spectral resolution ground level or airborne measurements.

CONCLUSION

This analysis is an attempt to improve our understanding of the relationships between canopy biophysical characteristics and the spectral shifts observed with high spectral resolution sensors. It is based on the coupling of leaf, canopy, and atmospheric radiative transfer models. Because of this, the results might be restricted to the assumptions and simplifications used in our modeling approach. Nevertheless, our findings are in good agreement with the experimental results reported in the literature. It appears that spectral shifts in the red edge are mainly produced by variations in chlorophyll concentration and leaf area index. The high spectral resolution index λ_i is quasi-independent of soil optical properties, irradiance conditions, or atmospheric effects when observed from space platforms. This is not the case for other high spectral resolution indices such as the first and second derivatives or even classical broad band vegetation indices. In contrast to the leaf scale, we have demonstrated that information provided by spectral shifts, observed on canopies, is not equivalent to broad band red and near-infrared reflectances. These interesting properties give some credit to the use of this spectral feature characteristic. However, the dynamic range of variation is not very large, and we have to be careful about the resulting signal to noise ratio, taking into account both the sensor noise and the algorithm used for evaluation of λ_i. However, compared to the noise expected on the second derivative at a given wavelength, as proposed by Hall et al. (1990), the spectral shift index should be better. Furthermore, when analyzing the huge amount of data provided by spectroimaging systems, the computing time is an important limiting factor. We propose a calculation method for λ_i, based on an *a priori* polynomial fitting of λ_i to a set of wavebands. It is not very time-consuming and quite accurate if three or more spectral bands in the red edge are used.

These simulations results need to be compared and validated with more experiments conducted either at ground level or from airborne platforms. The use of the high spectral resolution capabilities of the new generation of spectroimaging systems cannot be restricted to the red edge. We have demonstrated that spectral shifts are expected in other domains since other edges of chlorophyll or water specific absorption coefficients exist. As the architectural organization of the canopies affects the radiometric response over the whole spectrum, a more mechanistic approach where all the spectral domains are simultaneously and synergistically used is required.

This study has been supported by the French National Program for Remote Sensing in 1990. We thank X. F. Gu (INRA Bioclimatologie, Montfavet), J. Chadoeuf (INRA Biometrie, Montfavet), and M. D. Steven (Nottingham University) for their valuable advice and comments.

REFERENCES

Baret, F., Champion, I., Guyot, G., and Podaire, A. (1987), Monitoring wheat canopies with a high spectral resolution radiometer, *Remote Sens. Environ.* 22:367–378.

Baret, F. (1988), Un modèle simplifié de réflectance et d'absorptance d'un couvert végétal, in *Proc. 4ieme Coll. Int. Signatures Spectrules d'Objets en Télédétection*, Aussois (France), 18–22 January, ESA-SP 287, pp. 113–120.

Baret, F., and Guyot, G. (1991), Potentials and limits of vegetation indices, *Remote Sens. Environ.* 35:161–173.

Belanger, M. J. (1990), A seasonal perspective of several leaf developmental characteristics as related to the red edge of plant leaf reflectance, Ph.D. thesis, York University, Ontario, Canada, 110 pp.

Bonham-Carter, G. F. (1988), Numerical procedures and computer program for fitting an inverted gaussian model to vegetation reflectance data, *Comput. Geosci.* 14(3): 339–356.

Boochs, F., Kupfer, G., Dokter, K., and Kühbauch, W. (1990), Shape of the red edge as vitality indicator for plants, *Int. J. Remote Sens.* 11(10):1741–1753.

Bowers, S. A., and Hanks, R. J. (1965), Reflection of radiant energy from soils, *Soil Sci.* 100:130–138.

Campbell, G. S. (1986), Extinction coefficients for radiation in plant canopies calculated using ellipsoidal inclination angle distributions, *Agric. Forest Meteorol.* 36:317–321.

Chang, S. H., and Collins, W. (1983), Confirmation of the airborne biogeophysical mineral exploration technique using laboratory methods, *Econ. Geol.* 78:723–736.

Charles-Edwards, D. A. (1982), *Physiological Determinants of Crop Growth*. Academic, New York. 161 pp.

Collins, W., Chang, S. H., Raines, G., Canney, F., and Ashley, R. (1983), Airborne biogeophysical mapping of hidden mineral deposits, *Econ. Geol.* 78:737–749.

Conel, J. E., Adams, S., Alley, R. E., Hoover, G., and Schultz, S. (1988), AIS radiometry and the problem of contamination from mixed spectral orders, *Remote Sens. Environ.* 24:179–200.

Curran, P. J., Dungan, J. L., Macler, B. A., and Plummer, S. E. (1991), The effect of a red leaf pigment on the relationship between red edge and chlorophyll concentration, *Remote Sens. Environ.* 35:69–76.

Curran, P. J., Dungan, J. L., and Gholz, H. L. (1990), Exploring the relationship between reflectance red-edge and chlorophyll content in slash pine, *Tree Physiol.* 7:33–48.

Demetriades-Shah, T. H., and Steven, M. D. (1988), High spectral resolution indices for monitoring crop growth and chlorosis, in *Proc. 4th Int. Coll. on Spectral Signatures of Objects in Remote Sensing,* Aussois (France), 18–22 January, ESA SP-287, pp. 299–302.

Demetriades-Shah, T. H., Steven, M. D., and Clark, J. A. (1990), High resolution derivative spectra in remote sensing, *Remote Sens. Environ.* 33:55–64.

Ferns, D. C., Zara, S. J., and Barber, J. (1984), Application of high resolution spectroradiometry to vegetation, *Photogramm. Eng. Remote Sens.* 50(12):1725–1735.

Gates, D. M., Keegan, H. J., Schleter, J. C., and Weidner, V. R. (1965), Spectral properties of plants, *Appl. Opt.* 4(1): 11–20.

Gauthier, R. P., and Neville, R. A. (1985), Narrow-band multispectral imagery of the vegetation red reflectance edge for use in geobotanical remote sensing, in *Proc. 3rd Int. Coll. on Spectral Signatures of Objects in Remote Sensing,* Les Arcs (France), 16–20 December, ESA SP-247, pp. 233–236.

Guyot, G., Baret, F., and Jacquemoud, S. (1991), Imaging spectroscopy for vegetation studies, in *Imaging Spectroscopy: Fundamentals and Prospective Applications* (F. Toselli and J. Bodechtel, Eds.), Kluwer Academic, Dordrecht, The Netherlands.

Hall, F. G., Huemmrich, K. F., and Goward, S. N. (1990), Use of narrow-band spectra to estimate the fraction of absorbed photosynthetically active radiation, *Remote Sens. Environ.* 32:47–54.

Horler, D. N. H., Dockray, M., and Barber, J. (1983), The red edge of plant leaf reflectance, *Int. J. Remote Sens.* 4(2):273–288.

Jacquemoud, S., and Baret, F. (1990), PROSPECT: a model of leaf optical properties spectra, *Remote Sens. Environ.* 34:75–91.

Leprieur, C. E. (1989), Preliminary evaluation of AVIRIS airborne measurements for vegetation, in *Proc. 9th EARSeL Symp.*, Espoo Finland, 27 June–1 July 1989, pp. 524–530.

Miller, J. R., Hare, E. W., Neville, R. A., Gauthier, R. P., McColl, D., and Till, S. M. (1985), Correlation of metal concentration with anomalies in narrow band multispectral imagery of the vegetation red reflectance edge, in *Proc. 4th Int. Symp. on Remote Sensing of Environ.*, Thematic Conference: Remote Sensing for Exploration Geology, San Francisco 1–4 April 1985, pp. 143–153.

Milton, N. M., and Mouat, D. A. (1989), Remote sensing of vegetation responses to natural and cultural environmental conditions, *Photogramm. Eng. Remote Sens.* 55(8): 1167–1173.

Price, J. C. (1990), On the information content of soil reflectance spectra, *Remote Sens. Environ.* 33:113–121.

Richardson, A. J., and Wiegand, C. L. (1977), Distinguishing vegetation from soil-background information, *Photogramm. Eng. Remote Sens.* 43:1541–1542.

Rock, B. N., Hoshizaki, T., and Miller, J. R. (1988), Comparison of in situ and airborne spectral measurements of the blue shift associated with forest decline, *Remote Sens. Environ.* 24:109–127.

Rock, B. N., Miller, J. R., Moss, D. M., Freemantle, J. R., and Boyer, M. J. (1990), Spectral characterization of forest damage occurring on Whiteface Mountain, NY—studies with the Fluorescence Line Imager (FLI) and ground-based spectrometers, in *SPIE 1990 Technical Symposium on Optical Engineering and Photonic in Aerospace Sensing,* Orlando 16–20 April.

Slater, P. N. (1986), Survey of multispectral imaging systems for Earth observations, in *Remote Sensing Yearbook 1986* (A. Cracknell and L. Hayes, Eds), Taylor Francis, London, pp. 141–163.

Stoner, E. R., and Baumgardner, M. F. (1985), Characteristic variations in reflectance of surface soils, *Soil Sci. Soc. Am. J.* 45:1161–1165.

Tanré, D., Deroo, C., Dahaut, P., et al. (1990), Description of a computer code to simulate the satellite signal in the solar spectrum: the 5S code, *Int. J. Remote Sens.* 11(4): 659–668.

Vanderbilt, V. C., Ustin, S. L., and Clark, J. (1988), Canopy geometry changes due to wind cause red edge spectral shift, in *Proc. of IGARSS '88 Symp.*, Edinburgh, 13–16 September, ESA SP-284, p. 835.

Verhoef, W. (1984), Light scattering by leaf layers with application to canopy reflectance modeling: the SAIL model, *Remote Sens. Environ.* 16:125–141.

Verhoef, W. (1985), Earth Observation modeling based on layer scattering matrices, *Remote Sens. Environ.* 17:165–178.

Wang, Y. P., and Jarvis, P. G. (1988), Mean leaf angles for the ellipsoidal inclination angle distribution, *Agric. Forest Meteorol.* 43:319–321.